BIOCHEMISTRY
including biophysical chemistry & molecular biology

Article

Synthesis and Evaluation of a Library of Fluorescent Dipeptidomimetic Analogues as Substrates for Modified Bacterial Ribosomes

Sandipan Roy Chowdhury, Pradeep S Chauhan, Larisa M Dedkova, Xiaoguang Bai, Shengxi Chen, POULAMI TALUKDER, and Sidney M. Hecht

Biochemistry, **Just Accepted Manuscript** • DOI: 10.1021/acs.biochem.6b00102 • Publication Date (Web): 06 Apr 2016

ACS Publications

Biochemistry is published by the American Chemical Society. 1155 Sixteenth Street N.W., Washington, DC 20036

Synthesis and Evaluation of a Library of Fluorescent Dipeptidomimetic Analogues as Substrates for Modified Bacterial Ribosomes

Sandipan Roy Chowdhury,[†] Pradeep S. Chauhan,[†] Larisa M. Dedkova,[†] Xiaoguang Bai,[†] Shengxi Chen,[†] Poulami Talukder and Sidney M. Hecht[*,†]

[†]Center for BioEnergetics, Biodesign Institute, and School of Molecular Sciences, Arizona State University, Tempe, AZ 85287, United States

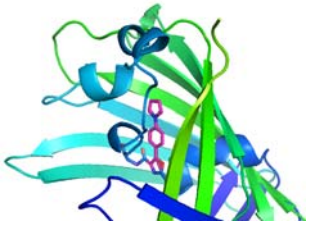

ABSTRACT: Described herein is the synthesis and photophysical characterization of a library of aryl substituted oxazole and thiazole based dipeptidomimetic analogues, and their incorporation into position 66 of green fluorescent protein (GFP) in lieu of the natural fluorophore. These fluorescent analogues resemble the fluorophore formed naturally by GFP. As anticipated, the photophysical properties of the analogues varied as a function of the substituents at the *para*-position of the phenyl ring. The maximum fluorescence emission wavelength of compounds in the library varied from ~365 nm (near UV region) to ~490 nm (visible region). The compounds also exhibited a large range of quantum yields (0.01 to 0.92). The analogues were used to activate a suppressor $tRNA_{CUA}$ and were incorporated into position 66 of GFP using an *in vitro* protein biosynthesizing system which employed engineered ribosomes selected for their ability to incorporate dipeptides. Four analogues with interesting photophysical properties and reasonable suppression yields were chosen and the fluorescent proteins (FPs) containing these fluorophores were prepared on a larger scale for more detailed study. When the FPs were compared with the respective aminoacyl-tRNAs and the actual dipeptide analogues, the FPs exhibited significantly enhanced fluorescence intensities at the same concentrations. Part of this was shown to be due to the presence of the fluorophores as an intrinsic element of the protein backbone. There were also characteristic shifts in the emission maxima indicating the environmental sensitivity of these probes. Acridon-2-ylalanine (Acd) and oxazole **1a** were incorporated into positions 39 and 66 of GFP, respectively, and were shown to form an efficient Förster resonance energy transfer (FRET) pair, demonstrating that the analogues can be used as FRET probes.

Fluorescent labeling of proteins and peptides can provide a powerful tool to monitor their behavior *in vitro* as well as *in vivo*.[1] Generally, fluorescent labeling is achieved by employing a derivative of the fluorophore that reacts specifically with certain functional groups present in the biomolecule.[2] Numerous fluorescent probes are currently available which possess a wide range of properties and functionalities to meet the requirements of the labeling technique and the technical goals of specific studies. There are, however, certain caveats associated with the use of synthetic fluorophores.[2] For example, they should be small in size and chemically stable under physiological conditions, they should not perturb the structure or function of the peptides/proteins being labeled, and when used in intact cells or organisms, they should not be cytotoxic and should be permeable to cell membranes. In addition, when used to measure protein conformational changes, the covalent linkage between the synthetic probe and the specific residue in the target molecule should provide the probe with a range of motion that is small relative to the change in protein conformation being monitored.[3]

Following the successful cloning of green fluorescent protein[4] (GFP) and its utilization as a marker for gene expression,[5] this application for GFP and its variants has been used widely.[6] There are certain advantages of genetic tagging over chemical labeling of expressed proteins.[7] For example, since the fluorescent protein is fused to the target protein, they are colocalized with absolute specificity, which obviates the problem of non-specific post-synthetic labeling. The fluorophore is embedded in the protein backbone and sheltered by the β-barrel structure, imparting a controlled environment for the probe. Nonetheless, there are significant limitations of using fluorescent proteins as labels, including their need for posttranslational activation, their limited stability and their large size.

Over a period of several years, we have reported the reengineering of *E. coli* ribosomes,

enabling them to incorporate α-D-amino acids[8,9] and β-amino acids,[10,11] while still incorporating α-L-amino acids with good fidelity. More recently, we have extended this strategy to the selection of ribosomes capable of incorporating dipeptides and dipeptide analogues from an activated suppressor tRNA into a specific site in a protein in a single ribosomal bond-forming event by suppression of a nonsense codon.[12,13] This has added importantly to the repertoire of amino acid analogues potentially amenable to incorporation, since the modified ribosomes apparently fail to recognize the amide bond connecting the two incorporated amino acids. Accordingly, the modified ribosomes were capable of incorporating a thiodipeptide, as well as fluorescent oxazole (**1a**) and thiazole (**8a**) heterocycles (Figure 1) substituted with NH_2 and COOH groups at distances which approximated those between such functional groups in a dipeptide.[12,13]

The structures of the dipeptidomimetic analogues incorporated were particularly interesting since they resemble the GFP fluorophore and are also fluorescent. When dipeptidomimetic analogues **1a** and **8a** were incorporated into position 66 of GFP by suppression of a UAG codon introduced into that position in lieu of the normal tyrosine codon, the resulting FPs had fluorescence intensities significantly stronger than wild-type GFP.[12,13] These dipeptidomimetic analogues do not require activation by posttranslational modification; further, they are completely stable chemically both as the free "dipeptides" and also as constituents of proteins. The success of these studies[12,13] suggested that it should be possible to identify additional fluorescent dipeptidomimetic analogues having diverse photophysical properties. Described in this report are the synthesis and photophysical properties of a library of dipeptidomimetic analogues and their ribosomal incorporation into position 66 of *Aequorea victoria* GFP. Selected fluorophores with interesting properties were made in greater amounts and characterized with

regard to their environmental sensitivity and ability to act as a FRET donor following incorporation into the β-barrel structural domain of GFP, using acridon-2-ylalanine (Acd)[14] as the acceptor.

MATERIALS AND METHODS

All experiments requiring anhydrous conditions were conducted in flame-dried glassware fitted with a rubber septum under a positive pressure of dry nitrogen or dry argon. Reactions were performed at room temperature unless otherwise indicated. Analytical thin layer chromatography was performed using glass plates pre-coated with silica gel (0.25 mm, 60 Å pore size, 230–400 mesh, Silicycle) impregnated with a fluorescent indicator (254 nm). TLC plates were visualized by exposure to ultraviolet (UV) light. Flash column chromatography was performed employing silica gel (60 Å pore size, 40–63 μm, standard grade, Silicycle). An acetone cooling bath was used for the appropriate low temperature reactions by the addition of portions of dry ice.

^{1}H NMR and ^{13}C NMR spectra were recorded on Varian INOVA 400 (400 MHz) and Varian INOVA 500 (500 MHz) spectrometers at 25 °C. Proton chemical shifts are expressed in parts per million (ppm, δ scale) and are referenced to residual protium in the NMR solvent ($CDCl_3$, DMSO-d_6 or CD_3OD). Splitting patterns are designated as follows: s, singlet; br s, broad singlet; d, doublet; dd, doublet of doublets; t, triplet; q, quartet; m, multiplet. High resolution mass spectra were obtained at the Arizona State University CLAS High Resolution Mass Spectrometry Facility or the Michigan State University Mass Spectrometry Facility. HPLC purification was performed with a Waters 600 pump coupled with a Varian ProStar 340 detector and a Grace Econosil C_{18} column (250 × 10 mm, 5 μm). The tetra-*n*-butylammonium (TBA) salt of pdCpA was prepared using Dowex 50W X8, 200–400 mesh, activated in its TBA form.

The chemicals used for synthesis were purchased from Aldrich Chemical Co., Sigma Chemical Co., Fisher Scientific, Oakwood Chemicals or Combi-Blocks. THF was distilled under argon using sodium-benzophenone ketyl; CH_2Cl_2 was distilled under argon using calcium hydride.

Synthesis of pdCpA Derivatives of Dipeptidomimetic Analogues. The route employed for the synthesis of the pdCpA derivative of dipeptidomimetic analogue **5a** and its attachment to suppressor $tRNA_{CUA}$-C_{OH} is outlined in Scheme 1. The syntheses of the pdCpA derivatives of dipeptidomimetics **2a**-**4a**, **6a**, **7a** and **9a**-**11a** are outlined in Schemes S1 to S8. The syntheses of the pdCpA derivatives of the dipeptidomimetic analogues **1a** and **8a**, and acceptor Acd have been reported previously.[12-14] The experimental procedures and compound characterizations are provided in the Supporting Information.

Methyl 3-(4-(1H-Pyrrol-1-yl)phenyl)-2-(2-((tert-butoxycarbonyl)amino)acetamido)-3-oxopropanoate (***17***)**.** To a solution of 0.83 g (4.41 mmol) of acid **13** in 25 mL of THF were added 1.59 mL (1.16 g, 18.6 mmol) of Et_3N and 0.74 mL (0.78 g, 9.31 mmol) of isobutyl chloroformate. The reaction mixture was stirred at room temperature for 2 h to obtain the acid anhydride **14**, which was used as a crude material in the next step without further purification.

To a solution of 1.17 g (4.63 mmol) of imine ester **15** in 100 mL of THF was added 4.63 mL (4.63 mmol) of 1 M NaHMDS solution in THF at –78 °C. After 30 min, the crude acid anhydride **14** was added to the reaction mixture, which was stirred at –78 °C for 2 h. The reaction mixture was quenched by the addition of conc HCl solution until pH ~ 2 was reached. The reaction mixture was concentrated under diminished pressure to obtain the amine salt **16** as a colorless solid which was used in the next reaction without further purification.

To a solution of 0.85 g (4.85 mmol) of Boc-Gly-OH in 30 mL of DMF were added 2.14 g (4.85 mmol) of BOP reagent and 0.67 mL (0.48 g, 4.85 mmol) of Et_3N. After 2 min, the amine salt **16**

dissolved in 20 mL of DMF was added to the reaction mixture, which was stirred overnight at room temperature. The reaction mixture was diluted with 300 mL of water and extracted with two 50-mL portions of EtOAc. The organic phase was dried ($MgSO_4$) and concentrated under diminished pressure. The residue was purified by chromatography on a silica gel column (10 × 4 cm). Elution with 1:1 hexanes–ethyl acetate gave the desired product **17** as a colorless foam: yield 1.06 g (58% overall yield from acid **13**); silica gel TLC R_f 0.50 (1:1 hexanes–ethyl acetate); ^{1}H NMR ($CDCl_3$) δ 1.44 (s, 9H), 3.71 (s, 3H), 3.93 (d, 2H, J = 4.0 Hz), 5.39 (br s, 1H), 6.21 (d, 1H, J = 8.0 Hz), 6.38-6.39 (m, 2H), 7.16-7.17 (m, 2H), 7.47 (d, 2H, J = 12.0 Hz) 7.60 (d, 1H, J = 8.0 Hz) and 8.17 (d, 2H, J = 8.0 Hz); ^{13}C NMR ($CDCl_3$) δ 28.5, 44.3, 53.5, 57.9, 80.5, 111.3, 119.1, 119.2, 119.4, 123.3, 130.8, 131.7, 131.8, 145.2, 150.7, 156.2, 167.2, 169.9 and 189.9; mass spectrum (APCI), m/z 416.1824 $(M+H)^+$ ($C_{21}H_{26}N_3O_6$ requires m/z 416.1822).

Methyl 5-(4-(1H-Pyrrol-1-yl)phenyl)-2-(((tert-butoxycarbonyl)amino)methyl)oxazole-4-carboxylate (**18**)**.** To a stirred solution of 0.23 g (0.88 mmol) of triphenylphosphine and 0.22 g (0.88 mmol) of iodine in 50 mL of CH_2Cl_2 was added 0.24 mL (0.17 g, 1.75 mmol) of Et_3N. The dark yellow solution was stirred for 5 min and 0.18 g (0.44 mmol) of ketoamide **17** was added to the reaction mixture, which was stirred at room temperature for 2 h. The reaction mixture was concentrated under diminished pressure and the residue was purified by chromatography on a silica gel column (10 × 1 cm). Elution with 1:1 hexanes–ethyl acetate gave the desired product **18** as a colorless solid: yield 0.11 g (63%); silica gel TLC R_f 0.50 (1:1 hexanes–ethyl acetate); ^{1}H NMR ($CDCl_3$) δ 1.45 (s, 9H), 3.91 (s, 3H), 4.51 (d, 2H, J = 8.0 Hz), 5.34 (br s, 1H), 6.34-6.35 (m, 2H), 7.11-7.13 (m, 2H), 7.42-7.45 (m, 2H) and 8.10-8.13 (m, 2H); ^{13}C NMR ($CDCl_3$) δ 28.5, 38.1, 53.6, 80.5, 111.4, 119.1, 119.3, 119.8, 120.2, 123.7, 123.7, 126.6, 128.1, 129.9, 142.0,

155.4, 155.7, 159.7 and 162.6; mass spectrum (APCI), *m/z* 398.1714 $(M+H)^+$ ($C_{21}H_{24}N_3O_5$ requires *m/z* 398.1716).

Methyl 5-(4-(1H-Pyrrol-1-yl)phenyl)-2-(pent-4-enamidomethyl)oxazole-4-carboxylate (**5b**)**.** To a solution of 0.20 g (0.55 mmol) of Boc-protected amine **18** in 10 mL of CH_2Cl_2 was added 10 mL of CF_3COOH. The reaction mixture was stirred overnight and concentrated under diminished pressure to afford the deprotected amine which was used in the next step without purification.

To the solution of deprotected amine in 15 mL of THF was added 0.11 g (0.55 mmol) of 4-pentenoyloxysuccinimide followed by 0.14 mL (0.10 g, 1.00 mmol) of Et_3N. The reaction mixture was stirred overnight at room temperature and then concentrated under diminished pressure. The residue was purified by chromatography on a silica gel column (10 × 1 cm). Elution with 1:10 MeOH–ethyl acetate gave the desired product **5b** as a colorless solid: yield 0.14 g (72%); silica gel TLC R_f 0.75 (1:10 MeOH–ethyl acetate); ^{1}H NMR ($CDCl_3$) δ 2.31-2.38 (m, 4H), 3.86 (s, 3H), 4.59 (d, 2H, J = 4.0 Hz), 4.92-5.03 (m, 2H), 5.76-5.78 (m, 1H), 6.31-6.32 (m, 2H), 6.82-6.85 (m, 1H), 7.08-7.09 (m, 2H), 7.38-7.41 (m, 2H) and 8.04-8.06 (m, 2H); ^{13}C NMR ($CDCl_3$) δ 29.5, 35.5, 36.6, 52.4, 111.4, 115.8, 119.0, 119.2, 119.3, 119.6, 122.9, 123.5, 126.4, 129.9, 131.6, 136.9, 142.0, 155.3, 159.4, 162.4 and 172.8; mass spectrum (APCI), *m/z* 380.1607 $(M+H)^+$ ($C_{21}H_{22}N_3O_4$ requires *m/z* 380.1610).

Cyanomethyl 5-(4-(1H-Pyrrol-1-yl)phenyl)-2-(pent-4-enamidomethyl)oxazole-4-carboxylate (**19**)**.** To a solution of 0.12 g (0.31 mmol) of ester **5b** in 6 mL of 1:1 MeOH and THF was added 0.46 mL (0.46 mmol) of 1 M aq LiOH. The reaction mixture was stirred

overnight at room temperature and then concentrated under diminished pressure to obtain the free acid.

To a solution of the acid in 15 mL of DMF was added 0.06 mL (0.07 g, 0.93 mmol) of chloroacetonitrile followed by 0.22 mL (0.16 g, 1.54 mmol) of Et_3N. The reaction mixture was stirred overnight at room temperature and then concentrated under diminished pressure. The residue was purified by chromatography on a silica gel column (10 × 1 cm). Elution with 1:10 MeOH–ethyl acetate gave the desired product **19** as a yellow solid: yield 70.0 mg (56%); silica gel TLC R_f 0.75 (1:10 MeOH–ethyl acetate); ^{1}H NMR ($CDCl_3$) δ 2.37-2.44 (m, 4H), 4.66 (d, 2H, J = 8.0 Hz), 4.95 (s, 2H), 4.97-5.10 (m, 2H), 5.80-5.84 (m, 1H), 6.27 (br s, 1H), 6.38-6.39 (m, 2H), 7.15-7.16 (m, 2H), 7.48-7.51 (m, 2H) and 8.11-8.14 (m, 2H); ^{13}C NMR ($CDCl_3$) δ 29.6, 35.7, 36.8, 49.1, 111.8, 114.3, 116.1, 119.2, 119.9, 122.9, 124.7, 130.0, 130.3, 137.0, 142.7, 157.4, 159.7, 160.6, 170.1 and 172.7; mass spectrum (APCI), *m/z* 405.1563 $(M+H)^+$ ($C_{22}H_{21}N_4O_4$ requires *m/z* 405.1563).

5-(4-(1H-Pyrrol-1-yl)phenyl)-2-(pent-4-enamidomethyl)oxazole-4-carboxylic acid pdCpA Ester (**20**). To a stirred solution containing 8.50 mg (6.37 μmol) of pdCpA tetrabutylammonium salt[15] in 100 μL of 9:1 anhydrous DMF–Et_3N was added 6.40 mg (15.9 μmol) of cyanomethyl ester **19**. The reaction mixture was sonicated for 6 h. The reaction mixture was purified by C_{18} reversed phase HPLC (250 × 10 mm) using a gradient of 1% to 65% acetonitrile in 50 mM ammonium acetate, pH 4.5, over a period of 1 h. The retention time of the desired product was 24.6 min. The fractions containing the product were lyophilized to afford **20** as a colorless solid: yield 2.0 mg (32%); mass spectrum (ESI), *m/z* 982.2283 $(M–H)^-$ ($C_{39}H_{42}N_{11}O_{16}P_2$ requires *m/z* 982.2286).

Measurement of the Photophysical Properties of Fluorescent Dipeptidomimetics. The UV/vis absorption spectra (220-400 nm) were recorded using a Cary 60 UV/vis spectrophotometer. Fluorescence quantum yields (Table 1) were determined using the gradient method.[16] Dipeptidomimetic analogues were dissolved in methanol. Solutions of each compound were made such that the UV absorptions at the maximum wavelength were within the range of 0.01 and 0.1. Anthracene (Φ_F 0.27, λ_{ex} 340 nm) was used as a reference standard to calculate the fluorescence quantum yields of the dipeptidomimetic analogues according to the formula $\Phi_x = \Phi_s \times (Grad_x \times n_x^2)/(Grad_s \times n_s^2)$, where *Grad* is gradient of the plot of integrated intensity versus absorbance, *n* is the refractive index of the solvent, *s* is the standard of known Φ_F, and *x* is the tested sample.[16]

Ligation of Suppressor $tRNA_{CUA}$-C_{OH} with Dipeptidomimetics and Deprotection of *N*-pentenoyl Group. The activation of suppressor $tRNA_{CUA}$ and $tRNA_{CCCG}$ was carried out as described previously.[17,18] Briefly, a 100-μL reaction mixture of 100 mM Na Hepes, pH 7.5, contained 1.0 mM ATP, 15 mM $MgCl_2$, 100 μg of suppressor $tRNA_{CUA}$-C_{OH} or $tRNA_{CCCG}$-C_{OH}, 0.5 A_{260} unit of *N*-pentenoyl-protected aminoacyl-pdCpA, 15% DMSO, and 100 units of T4 RNA ligase. The reaction mixture was incubated at 37 °C for 1.5 h and quenched by the addition of 0.1 vol of 3 M NaOAc, pH 5.2. The *N*-protected aminoacylated tRNA was precipitated with 3 vol of cold EtOH. The efficiency of ligation was estimated by 8% polyacrylamide–7 M urea gel electrophoresis (pH 5.0).[19] The *N*-pentenoyl-protected aminoacyl-$tRNA_{CUA}$s were deprotected by treatment with 5 mM aqueous I_2 at 25 °C for 15 min. The solution was centrifuged, and the supernatant was adjusted to 0.3 M NaOAc and then treated with 3 vol of cold EtOH to precipitate the aminoacylated tRNA. The tRNA pellet was collected by centrifugation, washed with 70% aq EtOH, air dried and dissolved in 10 μL of RNase-free H_2O.

Preparation of S-30 Extracts from Cells Having Modified Ribosomes. Aliquots (5-10 μL) from liquid stocks of *E. coli* BL-21(DE-3) cells, harboring plasmids with a wild-type or modified rrnB gene, were placed on LB agar supplemented with 100 μg/mL of ampicillin and grown at 37 ºC for 16-18 h. One colony was picked from each agar plate and transferred into 3 mL of LB medium supplemented with 100 μg/mL of ampicillin and 0.5 mM IPTG.

The cultures were grown at 37 ºC for 3-6 h in a thermostated shaker until OD_{600} ~0.15-0.3 was reached, then diluted with LB medium supplemented with 100 μg/mL ampicillin, 1 mM IPTG and 3 μg/mL of erythromycin (for selectively enhancing the modified ribosome fraction) until OD_{600} 0.01 was reached, and then grown at 37 ºC for 12-18 h. The optimal concentration of the final cultures was OD_{600} 0.5-1.0. Cells were harvested by centrifugation (5000 × g, 4 ºC, 10 min), washed three times with S-30 buffer (1 mM Tris-OAc, pH 8.2, containing 1.4 mM $Mg(OAc)_2$, 6 mM KOAc and 0.1 mM DTT) supplemented with β-mercaptoethanol (0.5 mL/L) and once with S-30 buffer having 0.05 mL/L β-mercaptoethanol.

The weight of the wet pellet was estimated and 1.27 mL of S-30 buffer was added to suspend each 1 g of cells. The volume of the suspension was measured and used for estimating the amount of other components. Pre-incubation mixture (0.3 mL) (0.29 M Tris, pH 8.2, containing 9 mM $Mg(OAc)_2$, 13 mM ATP, 84 mM phosphoenol pyruvate, 4.4 mM DTT and 5 μM amino acids mixture), 15 units of pyruvate kinase and 10 μg of lysozyme were added per 1 mL of cell suspension and the resulting mixture was incubated at 37 ºC for 30 min. The incubation mixture was then frozen at – 80 ºC (~30 min), melted (37 ºC, 30 min), and again frozen and melted at room temperature (~30 min). Ethylene glycol tetraacetic acid (EGTA) was then added to 2.5 mM final concentration and the cells were incubated at 37 ºC for 30 min. The same molar

concentration of $CaCl_2$ was added, mixed well and frozen (–80 ºC, 30 min). The frozen mixture was centrifuged (15,000 × g, 4 ºC, 1 h) and the supernatant was stored in aliquots at –80 ºC.

***In vitro* Protein Translation**. Protein translation reactions were carried out in 15-1700 μL of incubation mixture containing 0.3 μL/μL of S-30 system, 170 ng/μL of plasmid, 35 mM Tris acetate, pH 7.4, 190 mM potassium glutamate, 30 mM ammonium acetate, 2 mM DTT, 0.2 mg/mL total *E. coli* tRNA, 3.5% PEG 6000, 20 μg/mL folinic acid, 20 mM ATP and GTP, 5 mM CTP and UTP, 100 μM amino acids mixture, 0.5 μCi/μL of ^{35}S-methionine (for 15-μL reactions) and 1 μg/mL rifampicin. In the case of plasmids having a gene with a TAG codon, an activated suppressor tRNA was added to a concentration of 1.5 μg/μL. In the case of the plasmid having a gene with TAG and GGGC codons to enable the incorporation of two unnatural amino acids, two aminoacyl-tRNAs (aminoacyl-$tRNA_{CUA}$ and aminoacyl-$tRNA_{CCCG}$) were added. Reactions were carried out at 37 °C for 1 h (for 15 μL reaction mixtures) to 1.5 h (for 1700 uL reaction mixtures) and terminated by chilling on ice. Aliquots from *in vitro* translation mixtures were analyzed by SDS-PAGE followed by quantification of the radioactive bands by phosphorimager analysis (for 15 μL reaction mixtures).

Purification of GFP. Samples of GFP were diluted with 50 mM Tris-HCl, pH 8.2, and applied to a 100 μL Ni-NTA agarose column that had been equilibrated with the same buffer. The column was washed with 1 mL of the same buffer and GFP was eluted with 500 μL of the 50 mM Tris-HCl, pH 8.2, containing 250 mM imidazole. A 50-μL column of DEAE-Sepharose was equilibrated with two 500-μL portions of 25 mM Tris-HCl, pH 7.4. Samples of GFP purified by Ni-NTA chromatography were diluted 3-fold in the same buffer and applied to the resin. The column was washed with four 500-μL portions of the same buffer. GFP was eluted from the resin with 25 mM Tris-HCl, pH 7.4, containing 0.25 M NaCl. The fractions were analyzed on a

15% polyacrylamide gel, stained using Coomassie R-250, and protein-containing fractions were combined and concentrated by the use of an Amicon Ultra 10K filter device. The concentrations of all modified proteins were estimated by comparison with the corresponding wild-type proteins, which had been prepared *in vivo* and purified using the same protocols. The concentrations of the reference proteins were determined based on OD_{280} determination and the extinction coefficient for the protein. The wild-type protein of known concentration was then used as a reference standard at several concentrations in an SDS-PAGE experiment visualized by Coomassie staining in comparison with the modified proteins.

Protein Fluorescence Measurements. The fluorescence spectra of modified GFPs containing compounds **1a**, **3a**, **4a** and **8a** at positions 66, as well as compound **1a** at position 66 and Acd at position 39, were measured using a Varian Cary Eclipse Fluorescence Spectrophotometer with the excitation slit set at 10 nm and emission slit at 10 nm in 25 mM Tris-HCl, pH 7.4, containing 0.5 M NaCl.

The emission spectra of modified GFPs containing compounds **1a**, **3a**, **4a** and **8a** in position 66 were measured after excitation at appropriate wavelengths (300 nm for **1a** and **8a**; 320 nm for **3a**; 360 nm for **4a**). The emission spectra of the GFP analogue having Acd at position 39 and compound **1a** at position 66 were measured after excitation at two wavelengths (296 and 370 nm), corresponding to excitation maxima for compounds **1a** and Acd, respectively.

RESULTS

Synthesis of the Fluorescent Dipeptidomimetic Analogues and their pdCpA Esters.

The synthesis of the aminoacylated pdCpA derivative of dipeptidomimetic analogue **5a** (Figure 1) began with the conversion of commercially available 4-(1*H*-pyrrol-1-yl)benzoic acid

(**13**) to activated intermediate **14** by treatment with isobutylchloroformate and triethylamine (Scheme 1). This anhydride was condensed with the monoanion of the diphenylmethylene-glycine methyl ester (**15**), followed by imine hydrolysis using ~6 N HCl to afford amine salt **16**, which was used in the next step without further purification.[20] Amine salt **16** was coupled with Boc-Gly-OH using BOP[21] as a coupling agent to form α-amido-β-ketoester **17** in 58% overall yield from acid **13**. Cyclodehydration of **17** using triphenylphosphine in presence of iodine and triethylamine in CH_2Cl_2 afforded oxazole **18** in 63% yield.[20] Subsequent removal of the Boc group in **18** using CF_3COOH, followed by treatment with pentenoyloxysuccinimide gave the amide **5b** in 72% yield.[18] The methyl ester moiety of **5b** was saponified using ~1 N LiOH solution and the corresponding acid was activated as cyanomethyl ester **19** in 56% yield for two steps.[18,22] Treatment of cyanomethyl ester **19** with the tris(tetrabutylammonium) salt of pdCpA (TBA-pdCpA) in anhydrous DMF gave the corresponding aminoacylated pdCpA ester **20** in 32% yield.[15] Finally, activated pdCpA derivative **20** was ligated to an abbreviated suppressor $tRNA_{CUA}$-C_{OH} transcript using T4 RNA ligase, providing the respective misacylated suppressor tRNA transcript.

The syntheses of the aminoacylated pdCpA derivative of dipeptidomimetics **1a** and **8a** have been reported previously.[12,13] The synthesis of the pdCpA derivative of compound **2a** is described in Scheme S1 of the Supporting Information. The synthesis began with the condensation of commercially available 3,4,5-trimethoxybenzoyl chloride with the monoanion of the diphenylmethylene-glycine methyl ester (**15**), followed by imine hydrolysis using conc HCl to afford the hydrochloride salt of amine **21**. The latter was coupled directly with CBz-Gly-OSu in presence of triethylamine to form the α-amido-β-ketoester **22** in 79% overall yield from imine

15. The remaining steps for the synthesis of the pdCpA derivative of compound **2a** were similar to those described in Scheme 1.

The synthesis of the aminoacylated pdCpA derivative of oxazole **3a** (Scheme S2 of the Supporting Information) and the corresponding thiazole **9a** (Scheme S6 of the Supporting Information) began from known glycine derivative **26**.[23] Thus, fully protected glycine **26** was deprotonated using 1 M NaHMDS and condensed with 4-thiomethylbenzoyl chloride to obtain ketoester **27**. The Boc groups were removed from **27** using CF_3COOH followed by coupling with Boc-Gly-OH using the BOP reagent[21] to obtain α-amido-β-ketoester **28** in 72% overall yield from **26**. Cyclodehydration of **28** using triphenylphosphine in presence of iodine and triethylamine in CH_2Cl_2 gave oxazole **29** in 62% yield (Scheme S2 of the Supporting Information).[24] Treatment of **28** with the Lawesson's reagent gave the corresponding thiazole **47** in 87% yield (Scheme S6 of the Supporting Information).[20] The remaining steps for the synthesis of pdCpA derivatives of the oxazole dipeptidomimetic **3a** and the corresponding thiazole dipeptidomimetic **9a** were similar to those described in Scheme 1.

Similar reaction schemes were employed for the syntheses of the aminoacylated pdCpA derivatives of the oxazole dipeptidomimetics **4a**, **6a** and **7a**, and these are described in Schemes S3, S4 and S5, respectively, of the Supporting Information. Likewise, the reaction schemes for the synthesis of the aminoacylated pdCpA derivatives of the thiazole dipeptidomimetics **10a** and **11a** are shown in Schemes S7 and S8, respectively, of the Supporting Information.

Photophysical Properties of the Fluorescent Dipeptidomimetic Analogues. We characterized the photophysical properties of the library of oxazole and thiazole based dipeptidomimetic analogues, including molar absorptivities, quantum yields, emission and absorption spectra of the corresponding *N*-pentenoyl methyl ester derivatives in methanol (Table

1; Figure S1). Ideally, the photophysical data should have been measured in aqueous buffer to allow direct correlations with the same compounds present within a protein on attached to a tRNA. However, this was not possible due to the very limited solubility of some of the fluorophores in aqueous media. The absorbance maxima of the analogues ranged from 296 to 351 nm, while the emission maxima ranged from 365 to 490 nm. The photophysical properties of **1b** and **8b** have been described previously using samples having purity considered routine for synthetic products, although the careful purification of the compounds by reversed phase HPLC have now provided samples with reevaluated quantum yields.[12,13] The UV absorption and fluorescence emissions of **4b** and **10b** were the most red-shifted of the analogues studied. The emission peak wavelength of **10b** (490 nm) was closest to the emission peak wavelength of wild-type GFP (509 nm) with a large Stokes shift (139 nm). Nonetheless, **10b** proved to be a poor fluorescent probe since it has very low quantum yield (0.04). We verified (UV, HPLC analysis) that compound **10b** was unaltered chemically as a consequence of its excitation. Compound **4b** has quite favorable properties as a fluorescent probe. It has a high quantum yield (0.60) and high molar absorptivity (20000 M^{-1} cm^{-1}), emits in the blue region (458 nm) of the spectrum and has a large Stokes shift as compared with BFP (107 vs 75 nm). Compounds **3b** and **9b** were the best oxazole–thiazole pair in terms of quantum yield; both exhibited very high quantum yields, 0.92 and 0.91, respectively. Interestingly, the other oxazole-thiazole pairs differed significantly from each other in quantum yields; the thiazoles had significantly lower quantum yields compared to the corresponding oxazoles. This likely reflects the electron donating and withdrawing properties of the substituents by which these analogues differ. Apart from this, **3b** and **9b** emit in the visible region (419 and 447 nm, respectively), have large Stokes shifts (100 nm and 134 nm, respectively) and large molar absorptivities (21000 and 13100 M^{-1} cm^{-1}, respectively) which

make them efficient fluorescent probes. Although the absorption maximum of **2b** was similar to **1b**, the emission maximum was red-shifted by ~35 nm. The molar absorptivity of **2b** (14300 M^{-1} cm^{-1}) was roughly 80% that of **1b** (17600 M^{-1} cm^{-1}), such that the brightness of **2b** was less than that of **1b** (10600 vs 15800 M^{-1} cm^{-1}). In addition to **3b** and **9b**, which were quite bright (19300 and 12000 M^{-1} cm^{-1}, respectively), analogue **4b** also exhibited favorable brightness (12000 M^{-1} cm^{-1}). Compounds **5b**, **7b**, **10b** and **11b** exhibited one or more photophysical properties that diminish their brightness, and thus their potential utility as fluorescent probes.

Activation of Suppressor $tRNA_{CUA}$ and Synthesis of Modified GFPs. The individual *N*-pentenoyl protected aminoacylated pdCpA derivatives were ligated to an abbreviated suppressor $tRNA_{CUA}$-C_{OH} using T4 RNA ligase. The *N*-pentenoyl groups were removed using 5 mM aqueous I_2 at room temperature for 15 min. The free aminoacyl-tRNAs so obtained were then utilized in a cell free coupled transcription–translation system containing an *E. coli* S-30 preparation and pETGFP66 plasmid. The plasmid pETGFP66 contained a modified GFP gene having a TAG codon at position 66. As shown in Figure 2 and Table 2, the dipeptidomimetic analogues were all incorporated into GFP, but showed varying suppression efficiencies. In replicate experiments, the lowest suppression yield was ~3%, observed for compound **5a**, and the highest suppression yield was ~12%, observed for compound **4a**. Among the four oxazole/thiazole pairs (**1a**/**8a**; **3a**/**9a**; **4a**/**10a**; **6a**/**11a**), the best incorporation efficiency was shown by pair **4a** /**10a**. Compound **4a** was incorporated in ~12% yield and compound **10a** in ~10% yield. For the pairs **1a**/**8a,** and **3a**/**9a**, the suppression yields realized with the oxazoles were reproducibly higher than those observed for the corresponding thiazoles. Compounds **6a** and **11a** displayed roughly the same incorporation efficiencies, ~5% yields. Compounds **2a**, **5a** and **7a** were incorporated in ~6, ~3 and ~11% yields, respectively. Five of the analogues had

suppression yields ≥10%, which should enable quite reasonable quantities of proteins containing these analogues to be prepared. It may be noted that oxazole **1a** has previously been incorporated into DHFR in suppression yields up to 15%.[12]

Fluorescent Properties of the Oxazoles and Thiazoles, as tRNA Esters and Incorporated in Proteins and Peptides. GFP analogues having compounds **1a**, **3a**, **4a** and **8a** at position 66 were prepared on a larger scale and purified by Ni-NTA agarose chromatography. The fluorescence emission spectra of these modified GFPs were compared after excitation of each at the absorption maxima of the corresponding free fluorophores. The fluorescence emission maxima of proteins containing **1a**, **3a**, **4a** and **8a** were observed at shorter wavelengths (377, 410, 445 and 406 nm, respectively) than the emission maxima observed for the individual dipeptide analogues (cf Tables 1 and 3). It must be noted, however, that the monomeric fluorophores were investigated in MeOH, while the protein and activated tRNAs containing the same fluorophores were studied as aqueous solutions.

These emission wavelengths were characterized in more detail, by comparing the fluorescence emission spectra of analogues **1a**, **3a**, **4a** or **8a** present either at position 66 of GFP, or at the 3′-end of a suppressor tRNA. As shown in Figure 3, in which the concentrations of the activated tRNAs and GFPs had been adjusted to afford emission spectra of roughly comparable intensities, the emission maxima for the species containing **1a**, **3a** and **8a** differed by ~30-35 nm. In comparison, the emission spectrum of the activated tRNA and GFP containing **4a** differed by only 15 nm, and the emission spectrum of the activated tRNA was clearly narrower than that of the modified GFP.

The effect of environment on the fluorescence emission intensity of dipeptidomimetic analogue **1a** was studied by comparing the emission spectra of the free oxazole with those of the

corresponding aminoacyl-tRNA, and the modified GFP containing **1a** at position 66 (Figure 4). As shown, 100 nM free oxazole **1a** (green trace) and the same concentration of the suppressor tRNA activated with oxazole **1a** (orange trace) exhibited emission spectra of comparable intensity, with the emission maximum of the spectrum due to the activated tRNA being at longer wavelength (cf Table 3). In comparison, the modified GFP having **1a** at position 66 emitted at much shorter wavelength (377 nm) with several-fold greater intensity (Figure 4). The effect of solvent on the fluorescence emission wavelength and intensity of oxazole **1a** was also studied (Figure S2), and it was found that much of the observed differences in emission wavelength was due to the solvent. The slightly longer wavelength emission of the fluorophores attached to the 3′-end of tRNAs (e.g. Figure S2) presumably reflects a more polar environment induced by the tRNA, which contains multiple charged and polar functional groups.

The source of the enhanced fluorescence emission intensity observed for the modified GFP having **1a** at position 66 was explored by embedding oxazole **1a** in the tetrapeptide Gly-Gly-Gly-Gly to determine whether the simple presence of the fluorophore within a peptide backbone would influence its photophysical properties. The route used for the synthesis of the requisite peptide **12** is shown in Scheme 2, and that for the preparation of the requisite photophysical control (*N*-Boc **1a** methyl ester, **63**) is provided in Scheme S9. As noted in Table S1, the photophysical properties of Boc-deprotected peptide **12** differed in interesting ways from those of the analogously deprotected oxazole **63** (**1a** methyl ester). While both had the same absorption maxima when measured in MeOH (300 nm), the emission maximum of Boc-deprotected **12** was at shorter wavelength (381 vs 391 nm), analogous to the shifts observed when the oxazoles and thiazoles were present at position 66 of GFP (cf Table 3). Further, while their quantum yields were similar (0.88 and 0.92 for deprotected **12** and **63**, respectively), compound **12** may have

exhibited somewhat greater molar absorptivity, and consequently greater brightness than **63** (Table S1), although these differences were not statistically significant. The emission spectra of **12** and **63** were also recorded in MeOH, and reflected the same trends (Figure S3). When the same two Boc-deprotected compounds were studied in 25 mM Tris-HCl, pH 7.4, containing 0.5 M NaCl as had been done for the modified GFPs (Table 3), the overall differences in their photophysical properties were more pronounced (Table 4). The molar absorptivities and quantum yields decreased for both compounds, but the decrease in quantum yield was much greater for deprotected oxazole **63**. As a consequence deprotected **12** was more than three-fold brighter than deprotected **63** (Table 4). Once again, these trends were reflected in the fluorescence emission spectra of **63** and **12** themselves taken in the same buffer (Figure 5). Thus the several-fold differences in fluorescence intensity noted in Figure 4 must be due in part to the presence of the fluorophore as an intrinsic structural constituent of the protein backbone (rather than as the usual electronically isolated substituent attached to the peptide backbone), and in part to its additional presence within the β-barrel structure of GFP.

To explore the capability of the dipeptidomimetic analogues as FRET probes, we selected compound **1a** as the donor. The emission peak wavelength of **1a** after incorporation into position 66 of GFP was at 377 nm (Table 3). As the fluorescence acceptor we chose acridon-2-ylalanine (Acd) which has absorption peaks at 388 nm and 407 nm in water as a monomer, and emission peaks at ~420 and 450 nm. As position 66 is within the β-barrel structure of GFP, it was chosen for donor **1a** whereas position 39, outside of the β-barrel, was chosen for acceptor Acd. The spectral overlap between the fluorescence emission of oxazole **1a** and the absorption spectrum of Acd is shown in Figure S4. The predicted R_0 value for these two fluorophores was calculated[25] as 32.8 Å, while the distance between the α-carbon atoms of residues 39 and 66 is 17.0 Å based on

X-ray crystallography (Figure 6B). By decoding the four base codon CGGG with the acridon-2-ylalanyl-tRNA$_{CCCG}$ and the nonsense codon UAG with the oxazolyl-tRNA$_{CUA}$, Acd and compound **1a** were incorporated into GFP at positions 39 and 66, respectively. The incorporation yield was 5% compared to wild-type GFP. After purification, the doubly modified GFP was excited at 296 nm. As demonstrated in Figure 6A, the modified GFP containing fluorescence acceptor Acd at position 39 and compound **1a** at position 66 displayed a FRET signal at ~450 nm. The theoretical maximum intensity of the FRET peak is defined by the orange curve in Figure 6A, which shows the emission spectrum of Acd following its direct excitation by irradiation at 370 nm. A control experiment involving a GFP having glycine at position 66 and Acd at position 39 gave only weak emission at 450 nm when irradiated at 296 nm (Figure S5).

DISCUSSION

We have recently described the recognition by engineered bacterial ribosomes of suppressor tRNAs activated with dipeptide analogues containing oxazole and thiazole cores, and the incorporation of these heterocyclic species into dihydrofolate reductase and green fluorescent protein.[12,13] The incorporations have been verified by mass spectrometric analysis of tryptic digests of the modified proteins. The strongly fluorescent nature of the derived proteins prompted the preparation and study of a library of substituted oxazoles and thiazoles to enable a better understanding of the nature and scope of our initial observations. The synthesis of 1,3-oxazoles and 1,3-thiazoles has been the focus of many studies as a consequence of their widespread occurrence in natural products. Nature biosynthesizes oxazoles through cyclodehydration and oxidation of acylserine derivatives,[26] and many synthetic routes for oxazoles follow this general strategy.[27,28] Another versatile method for the synthesis of 1,3-

oxazoles involves the cyclodehydration of α-acylaminoketones, esters or amides;[29] the oxazole synthesis described in this report falls in this category. The α-amido-β-ketoesters were cyclized directly using a dehydrating mixture of two equivalent of triphenylphosphine, iodine and triethylamine,[24] and the reactions were typically complete within 15 minutes at room temperature.

There are also number of methods for the synthesis of 1,3-thiazoles, the most common involving the condensation of substituted α-haloketones and thioamides. In this report, the thiazoles were obtained by the cyclization of α-amido-β-ketoesters using Lawesson's reagent.[30] This method was followed since the α-amido-β-ketoester was a common intermediate for both oxazole and thiazole syntheses, which simplified the overall process of library construction.

Aequorea victoria GFP chromophore is formed by a dehydrative cyclization, involving the Tyr moiety at position 66 in the nascent polypeptide. The phenolic OH group of the Tyr moiety is particularly important for the photophysical properties of GFP.[31] There have been an extensive structure–activity studies of the GFP fluorophore. In addition, site-directed mutagenesis has enabled the mutation of GFP chromophore by Phe analogues with different *para*-substituents in place of Tyr66.[32,33] These studies indicated that the wavelength maxima for both absorption and emission peaks of GFP fluorophore increased with increasing electron-donating ability of these substituents. In order to build a library of the dipeptidomimetic analogues with a wide variety of photophysical properties, several oxazole and thiazole analogues containing either electron-donating (NMe_2, SMe, OMe) or electron-withdrawing (NO_2, pyrrole, CN) substituents were synthesized. The wavelength of emission peaks for both oxazoles and thiazoles were in the order NMe_2 > SMe > OMe ≈ NO_2 ≈ pyrrole > CN, i.e. roughly in the order predicted by studies of the GFP fluorophore. As the most electron-donating substituent the presence of NMe_2 elicited the

maximum red shift of the absorption and emission peaks. Compounds **4b** and **10b** both had absorption maxima at 351 nm and had emission maxima at 458 and 490 nm in methanol, respectively. Nitrile **6b** exhibited the shortest wavelength absorption and emission peaks (285 and 365 nm, respectively). Compound **2b** can be considered as a more electron dense congener of compound **1b** because it contains methoxyl groups at both *meta*-positions in addition to the one at the *para*-position. It was anticipated correctly that compound **2b** would exhibit a red shift in absorption and emission peak wavelengths compared to compound **1b**, although the shift was not dramatic, presumably due to the placement of the additional OMe groups at the *meta* positions. In all cases, the emission maxima of the thiazoles were ~20-30 nm red-shifted compared to the corresponding oxazoles. The molar absorptivity values for the oxazoles were also greater compared to the corresponding thiazoles. Similarly, the quantum yields for the oxazoles were generally greater than for the corresponding thiazoles, with the exception of compounds **3b** and **9b**, both of which exhibited very high quantum yields. In comparison, the compounds having electron-withdrawing substituents (**5b**, **6b**, **7b** and **11b**) displayed very low quantum yields.

In order to study the basis for the observed photophysical properties of the oxazoles and thiazoles, four compounds (**1b**, **3b**, **4b** and **8b**) were used to prepare the respective activated suppressor tRNAs and modified GFPs on a larger scale. As shown in Table 3 and Figure 4, when these compounds were incorporated at the 3′-end of tRNAs as activated esters, the fluorescence emission maxima were generally shifted to longer wavelength, albeit without any significant increase in fluorescence intensity. In contrast, when the four compounds were incorporated into position 66 of GFP the resulting GFP analogues had several-fold stronger fluorescent intensities

than the free compounds and the corresponding aminoacyl-tRNA$_{CUAS}$, and the fluorescence emission occurred at shorter wavelengths in each case (Figures 3 and 4).

The oxazoles and thiazoles employed in the current study are unique as synthetic protein fluorophores in that the conjugated systems which are responsible for their fluorescent properties actually become part of the polypeptide/protein backbone. Accordingly, it seemed possible that the effects noted in Table 3, and Figures 3 and 4, related to alterations of fluorescence intensity and emission wavelength maxima, might be influenced by the simple incorporation of these fluorophores into a polypeptide. As shown in Table 4 and Figure 5, this is clearly the case. Embedding oxazole **1a** within the tetrapeptide Gly-Gly-Gly-Gly caused its fluorescence emission wavelength maximum to shift to shorter wavelength (from 407 to 399 nm), as also noted for the oxazoles and thiazoles incorporated at position 66 of GFP (cf Table 3). The embedded oxazole also exhibited about a three-fold greater brightness of its fluorescence signal as compared with the free oxazole when measured in Tris-HCl buffer (Table 4). This increase in brightness was associated with an increased quantum yield, plausibly due to suppression of non-radiative deactivation pathways by the rigid peptide matrix. This observation parallels an earlier finding[12] in which we noted that the incorporation of oxazole **1a** at position 39 of GFP (outside the β-barrel structure) produced a stronger emission than that observed for free oxazole **1b**. Inclusion of the embedded oxazole at position 66 (which is within the β-barrel structure, Figure 6B) effected a further enhancement in fluorescence emission intensity. More specifically, we found that the absorption extinction coefficient for GFP containing **1a** at position 39 was 50,200 M^{-1} cm^{-1}, while that for GFP itself was 25,000.[12] The quantum yield for the GFP analogues containing **1a** at position 39 was 0.84 vs 0.79 for GFP itself. When **1a** was present at position 66 of GFP, the absorption extinction coefficient was 90,300 M^{-1} cm^{-1} and the quantum yield was

0.91. Thus introducing **1a** at position 39 of GFP produced a protein about two-fold brighter than native GFP, while introducing this fluorophore at position 66 resulted in a protein about four-fold brighter than wild-type GFP.[12] This change was associated with a change in the absorption extinction coefficient of **1b**. Embedding oxazole **1a** in GFP at position 66 enhanced its brightness ~25 to 30-fold. It is worth noting that our novel GFP, having **1** at position 66, is also two- to three-fold brighter than a "class 2" GFP[34] having an absorption extinction coefficient about twice that of GFP that we employed for modification. While oxazole **1a** is roughly isosteric with a dipeptide, and has been introduced into the β-barrel structure in lieu of a single amino acid (Tyr66), there appears to be ample room within the β-barrel structure to accommodate this larger molecular entity (Figure 6B). Finally, the much smaller Stokes shift observed for oxazole **1a** within the β-barrel of GFP[12] may reasonably be attributed to a suppression of solvent relaxation. While the environmental sensitivity of these fluorophores should provide the wherewithal for enhanced definition of the microenvironment of proteins and proteins complexes, there will also be a corresponding increase in the complexity of quantification as a consequence of the aforementioned environmental sensitivity.

We conclude that the significant observed changes in emission wavelength and intensity are due both to incorporation of the fluorophore within the protein backbone, and also to the environmental sensitivity of these fluorophores, and that this property may potentially be exploited to utilize such compounds as reporters of their environment, and conformational changes which alter that environment. It may be noted that the introduction of oxazole **1a** into position 39 of GFP, which is not within the β-barrel structure, afforded a much more significant increase in fluorescence intensity of the oxazole[12] than did its present inclusion within a tetraglycine peptide. Accordingly, it might be anticipated that alteration of peptide structure, e.g.

by the inclusion of aromatic or lipophilic amino acids, would also affect the brightness of the embedded oxazole.

Fluorescent proteins have been used as probes of molecular assembly in FRET experiments,[35] although their large size does impose constraints on the utility of this approach. The environmental sensitivity of the oxazoles and thiazoles studied here, as well as their small size, chemical stability and stronger fluorescence as compared with natural GFPs,[36] suggests that they may have superior potential as reporter groups. Accordingly, we prepared a modified GFP having a strong oxazole fluorophore at position 66 within the β-barrel structure, and a fluorescence acceptor (Acd) whose absorption spectrum overlaps the emission spectrum of the oxazole outside the β-barrel at position 39. The R_0 value of this potential FRET pair was calculated[25] as 32.8 Å, while the distance calculated from an X-ray crystal structure[37] was 17.0 Å (Figure 6B). As predicted, when the doubly modified GFP was irradiated at the excitation maximum of the oxazole at position 66 (296 nm), a FRET peak was evident (Figure 6A).

Where spectral overlap exists, the R_0 value for a given FRET pair increases in direct proportion to the quantum yield of the donor fluorophore and molar absorptivity of the acceptor. Given the very favorable molar absorptivities and quantum yields of many of the novel fluorophores studied here, as well as their environmental sensitivity and ability to be incorporated into proteins with reasonable suppression efficiencies, it is anticipated that they may find utility as reporter groups in experiments involving protein conformation and binding interactions with other (macro)molecules. Further, the activated tRNAs whose fluorescence emission properties are summarized in Table 3 may plausibly be of utility in reporting on the environment of the aminoacyl moiety during the partial reactions of protein biosynthesis. Presumably, such

interactions may be unique to protein biosynthesizing systems in which the ribosomes have been modified to accommodate dipeptidyl-tRNAs as substrates.

It should be noted that the present experiments were all carried out in cell free systems, and application of the present artificial fluorescent proteins in a cellular context would require significant extensions of the current technology.

CONCLUSIONS

A library of several fluorescent oxazole- and thiazole-based dipeptidomimetic analogues has been synthesized. The analogues are structurally similar to the GFP chromophore, but are stable chemically and do not require activation to exhibit fluorescence. In order to encompass a variety of photophysical properties, the compounds were designed with different electron-donating and electron-withdrawing substituents at the position analogous to the *p*-OH group in the GFP fluorophore. The compounds displayed reasonable efficiency of incorporation into position 66 of GFP using modified ribosomes and misacylated suppressor $tRNA_{CUA}$s. In addition, four mutant GFPs each containing a dipeptide analogue with favorable fluorescent properties and formed in good suppression yield were prepared in larger quantities and were characterized in more detail. All of the modified GFPs exhibited several-fold higher fluorescence intensities compared to the corresponding aminoacyl $tRNA_{CUA}$s, and were more strongly fluorescent than GFP itself. The fluorescent properties (emission wavelength and intensity) were shown to be responsive to environment, both within the protein backbone and especially within a secondary structure such as a β-barrel. Embedding the oxazole within a simple tetrapeptide also enhanced the intensity of its fluorescence emission. A successful FRET experiment demonstrated the potential utility of the fluorophores as reporter groups to monitor protein conformational changes and molecular interactions.

ASSOCIATED CONTENT

Supporting Information

The Supporting Information is available free of charge on the ACS Publications website at DOI

AUTHOR INFORMATION

Corresponding Author

* Email: sidney.hecht@asu.edu. Phone: (480) 965-6625. Fax: (480) 965-0038.

Funding

This study was supported by Research Grant GM 103861 from the National Institute of General Medical Sciences, National Institutes of Health.

Notes

The authors declare no competing financial interest.

ABBREVIATIONS

APCI, atmospheric pressure chemical ionization; ESI, electrospray ionization; GFP, green fluorescent protein; FP, fluorescent protein; HPLC, high-performance liquid chromatography; TLC, thin layer chromatography; DMSO, dimethylsulfoxide; R_f, ratio of fronts; Hz, Hertz; THF, tetrahydrofuran; DMF, dimethylformamide; TBA, tetrabutylammonium; BOP, *N*-[oxytris(dimethylamino)phosphonium]benzotriazole hexafluorophosphate; EGTA, ethylene glycol tetraacetic acid; PEG, polyethylene glycol; SDS-PAGE, sodium dodecyl sulfate–polyacrylamide gel electrophoresis; Ni-NTA, nickel nitrilotriacetic acid; DIPEA, diisopropylethylamine; UV, ultraviolet.

REFERENCES

(1) Chen, I., and Ting, A. Y. (2005) Site-specific labeling of proteins with small molecules in live cells. *Curr. Opin. Biotechnol. 16*, 35–40.

(2) Sahoo, H. (2012) Fluorescent labeling techniques in biomolecules: a flashback. *RSC Adv. 2*, 7017–7029.

(3) Chen, S., Fahmi, N. E., Wang, L., Bhattacharya, C., Benkovic, S. J., and Hecht, S. M. (2013) Detection of dihydrofolate reductase conformational change by FRET using two fluorescent amino acids. *J. Am. Chem. Soc. 135*, 12924–12927.

(4) Heim, R., Prasher, D. C., and Tsien, R. Y. (1994) Wavelength mutations and posttranslational autoxidation of green fluorescent protein. *Proc. Natl. Acad. Sci. U.S.A. 91*, 12501–12504.

(5) Chalfie, M., Tu, Y., Euskirchen, G., Ward, W. W., and Prasher, D. C. (1994) Green fluorescent protein as a marker for gene expression. *Science 263*, 802–805.

(6) Walker, C. L., Lukyanov, K. A., Yampolsky, I. V., Mishin, A. S., Bommarius, A. S., Duraj-Thatte, A. M., Azizi, B., Tolbert, L. M., and Solntsev, K. M. (2015) Fluorescence imaging using synthetic GFP chromophores. *Curr. Opin. Chem. Biol. 27*, 64–74.

(7) Marks, K. M., and Nolan, G. P. (2006) Chemical labeling strategies for cell biology. *Nature Methods 3*, 591–596.

(8) Dedkova, L. M., Fahmi, N. E., Golovine, S. Y., and Hecht, S. M. (2003) Enhanced D-amino acid incorporation into protein by modified ribosomes. *J. Am. Chem. Soc. 125*, 6616–6617.

(9) Dedkova, L. M., Fahmi, N. E., Golovine, S. Y., and Hecht, S. M. (2006) Construction of modified ribosomes for incorporation of D-amino acids into proteins. *Biochemistry 45*, 15541–15551.

(10) Dedkova, L. M., Fahmi, N. E., Paul, R., del Rosario, M., Zhang, L., Chen, S., Feder, G., and Hecht, S. M. (2012) β-Puromycin selection of modified ribosomes for *in vitro* incorporation of β-amino acids. *Biochemistry 51*, 401–415.

(11) Maini, R., Nguyen, D. T., Chen, S., Dedkova, L. M., Chowdhury, S. R., Alcala-Torano, R., and Hecht, S. M. (2013) Incorporation of β-amino acids into dihydrofolate reductase by ribosomes having modifications in the peptidyltransferase center. *Bioorg. Med. Chem. 21*, 1088–1096.

(12) Maini, R., Dedkova, L. M., Paul, R., Madathil, M. M., Chowdhury, S. R., Chen, S., and Hecht, S. M. (2015) Ribosome-mediated incorporation of dipeptides and dipeptide analogues into proteins in vitro. *J. Am. Chem. Soc. 137*, 11206–11209.

(13) Roy Chowdhury, S., Maini, R., Dedkova, L. M., and Hecht, S. M. (2015) Synthesis of fluorescent dipeptidomimetics and their ribosomal incorporation into green fluorescent protein. *Bioorg. Med. Chem. Lett. 25*, 4715–4718.

(14) Talukder, P., Chen, S., Liu, C. T., Baldwin, E. A., Benkovic, S. J., and Hecht, S. M. (2014) Tryptophan-based fluorophores for studying protein conformational changes. *Bioorg. Med. Chem. 22*, 5924–5934.

(15) Robertson, S. A., Noren, C. J., Anthony-Cahill, S. J., Griffith, M. C., and Schultz, P. G. (1989) The use of 5'-phospho-2 deoxyribocytidylylriboadenosine as a facile route to chemical aminoacylation of tRNA. *Nucleic Acids Res. 17*, 9649–9660.

(16) Lakowicz, J. R. (1983) *Principles of Fluorescence Spectroscopy*, Plenum Press.

(17) Lodder, M., Golovine, S., and Hecht, S. M. (1997) A chemical deprotection strategy for the elaboration of misacylated transfer RNA's. *J. Org. Chem. 62*, 778–779.

(18) Lodder, M., Golovine, S., Laikhter, A. L., Karginov, V. A., and Hecht, S. M. (1998) Misacylated transfer RNAs having a chemically removable protecting group. *J. Org. Chem. 63*, 794–803.

(19) Varshney, U., Lee, C. P., and RajBhandary, U. L. (1991) Direct analysis of aminoacylation levels of tRNAs in vivo. Application to studying recognition of *Escherichia coli* initiator tRNA mutants by glutaminyl-tRNA synthetase. *J. Biol. Chem. 266*, 24712–24718.

(20) Sanz-Cervera, J. F., Blasco, R., Piera, J., Cynamon, M., Ibanez, I., Murguia, M., and Fustero, S. (2009) Solution versus fluorous versus solid-phase synthesis of 2,5-disubstituted 1,3-azoles. Preliminary antibacterial activity studies. *J. Org. Chem. 74*, 8988–8996.

(21) Castro, B., Dormoy, J. R., Evin, G., and Selve, C. (1975) Peptide coupling reagents. IV. N-[Oxytris(dimethylamino)phosphonium]benzotriazole hexafluorophosphate. *Tetrahedron Lett. 16*, 1219–1222.

(22) Robertson, S. A., Ellman, J. A., and Schultz, P. G. (1991) A general and efficient route for chemical aminoacylation of transfer RNAs. *J. Am. Chem. Soc. 113*, 2722–2729.

(23) Kometani, M., Ihara, K., Kimura, R., and Kinoshita, H. (2009) Stereoselective syntheses of (E)-α,β-didehydroamino acid and peptide containing its residue utilizing oxazolidinone derivative. *Bull. Chem. Soc. Jpn. 82*, 364–380.

(24) Wipf, P., and Miller, C. P. (1993) A new synthesis of highly functionalized oxazoles. *J. Org. Chem. 58*, 3604–3606.

(25) Speight, L. C., Muthusamy, A. K., Goldberg, J. M., Warner, J. B., Wissner, R. F., Willi, T. S., Woodman, B. F., Mehl, R. A., and Petersson, E. J. (2013) Efficient synthesis and in vivo incorporation of acridon-2-ylalanine, a fluorescent amino acid for lifetime and Förster resonance

energy transfer/luminescence resonance energy transfer studies. *J. Am. Chem. Soc. 135,* 18806–18814.

(26) Li, Y.-M., Milne, J. C., Madison, L. L., Kolter, R., and Walsh, C. T. (1996) From peptide precursors to oxazole and thiazole-containing peptide antibiotics: microcin B17 synthase. *Science 274*, 1188–1193.

(27) Sakakura, A., Kondo, R., Umemura, S., and Ishihara, K. (2009) Dehydrative cyclization of serine, threonine and cysteine residues catalyzed by molybdenum(VI) oxo compounds. *Tetrahedron 65*, 2102−2109.

(28) Meyers, A. I., and Tavares, F. X. (1996) Oxidation of oxazolines and thiazolines to oxazoles and thiazoles. Application of the Kharasch-Sosnovsky reaction. *J. Org. Chem. 61*, 8207−8215.

(29) Robinson, R. (1910) New synthesis of oxazole derivatives. *Proc. Chem. Soc., London 25*, 295−296.

(30) Thomsen, I., Pedersen, U., Rasmussen, P. B., Yde, B., Andersen, T. P., and Lawesson, S. O. (1983) Studies on organophosphorus compounds. XLIV. Novel and convenient methods for the preparation of substituted thiophenes, thiazoles, and 1,3,4-thiadiazole-2(3H)-thiones from bifunctional substrates. *Chem. Lett. 12*, 809–810.

(31) Tolbert, L. M., Baldridge, A., Kowalik, J., and Solntsev, K. M. (2012) Collapse and recovery of green fluorescent protein chromophore emission through topological effects. *Acc. Chem. Res. 45*, 171–181.

(32) Wang, L., Xie, J., Deniz, A. A., and Schultz, P. G. (2003) Unnatural amino acid mutagenesis of green fluorescent protein. *J. Org. Chem. 68*, 174–176.

(33) Kajihara, D., Hohsaka, T., and Sisido, M. (2005) Synthesis and sequence optimization of GFP mutants containing aromatic non-natural amino acids at the Tyr66 position. *Prot. Eng. Des. Sel. 18*, 273–278.

(34) Tsien, R. Y. (1998) The green fluorescent protein. *Annu. Rev. Biochem. 67*, 509–544.

(35) Piston, D. W., and Kremers, G.-J. (2007) Fluorescent protein FRET: the good, the bad and the ugly. *Trends Biochem. Sci. 32*, 407–414.

(36) Shaner, N. C., Patterson, G. H., and Davidson, M. W. (2007) Advances in fluorescent protein technology. *J. Cell Sci. 120*, 4247–4260.

(37) Yang, F., Moss, L. G., and Phillips, G. N. Jr. (1996) The molecular structure of green fluorescent protein. *Nat. Biotechnol. 14*, 1246–1251.

Table 1. Photophysical Properties of the Dipeptidomimetic Analogues[a]

Analogue	Structure	λ_{abs} (nm)	λ_{em} (nm)	ε ($M^{-1}cm^{-1}$)	Φ_F	Brightness
1b	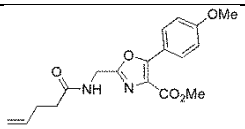	296±2	389±2	17600±1000	0.90±0.02	15800±1300
2b	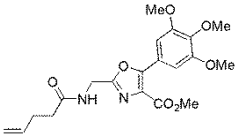	302±2	425±2	14300±900	0.72±0.02	10300±930
3b	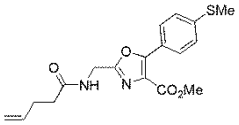	319±3	419±2	21000±1000	0.92±0.03	19300±1500
4b	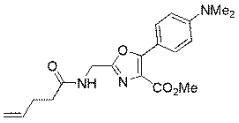	351±2	458±2	20000±1200	0.60±0.02	12000±1100
5b	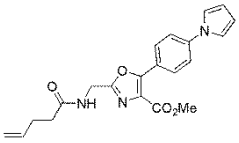	314±2	401±3	27900±1000	0.03±0.001	840±60
6b	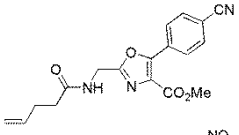	285±2	365±3	13800±1100	0.26±0.01	3600±400
7b	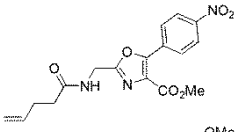	309±3	410±4	16200±1000	0.01±0.001	160±25
8b	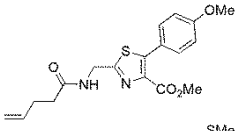	300±2	420±3	11000±1000	0.24±0.03	2600±500
9b	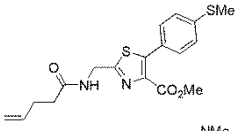	313±2	447±2	13100±900	0.91±0.04	12000±1400
10b	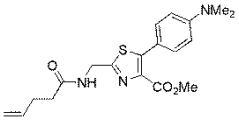	351±2	490±2	7500±500	0.04±0.001	300±30
11b	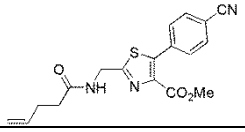	290±3	389±5	9500±500	0.01±0.001	95±15

[a]Determined for the N-pentenoyl-protected methyl esters in MeOH.
[b]Following excitation at the aborption maxima.

Table 2. Summary of Incorporation of Compounds 1a-11a into position 66 of GFP in Comparison with the Incorporation of Tyrosine

Average yield of full size protein in the presence of tRNA, containing fluorescent compounds, %											
Tyr[a]	**1a**	**2a**	**3a**	**4a**	**5a**	**6a**	**7a**	**8a**	**9a**	**10a**	**11a**
100	11±1	6±0.2	10±1	12±2	3±1	6±1	11±2	8±1	6±1	10±1	4±2

[a]The efficiency of full length GFP synthesis in the presence of tyrosyl-tRNA was ~40-60% of wild-type GFP synthesis under the same conditions.

Table 3. **Comparison of Emission Wavelengths (λ_{max}) of Free Dipeptidomimetic Compounds and the Same Compounds, Esterified to tRNA and Incorporated into Position 66 of GFP**[a]

Compound	Maximum emission wavelength (λ_{max}), nm		
	Free compound	Esterified to tRNA	Position 66 of GFP
1a	389±2	411±3	377±3
2a	425±2	450±2	
3a	419±2	445±2	410±2
4a	458±2	460±2	445±2
5a	401±3	420±3	
6a	365±3	370±3	
7a	410±4	420±4	
8a	420±3	435±2	406±2
9a	447±2	470±2	
10a	490±2	490±2	
11a	389±5	405±4	

[a]The emission spectra of the free oxazoles/thiazoles **1b – 11b** were determined in MeOH, while those of the activated tRNAs and GFPs were measured in 25 mM Tris-HCl, pH 7.4, containing 0.25 M NaCl.

Table 4. Photophysical Properties of the Free amines Derived from Compounds 12 and 63[a,b]

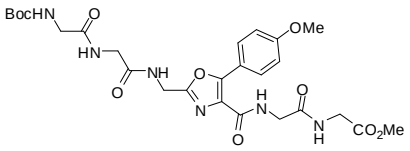

12

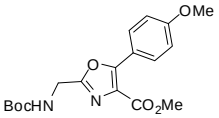

63

Compound	λ_{abs} (nm)	λ_{em} (nm)	ε ($M^{-1}cm^{-1}$)	Φ_F	Brightness
12	295±2	399±2	14100±1000	0.69±0.04	9700±1250
63	295±2	407±3	12500±1000	0.25±0.02	3100±500

[a]Determined in in 25 mM Tris-HCl, pH 7.4, containing 0.5 M NaCl. [b]Both compounds were treated with CF_3COOH to remove the Boc protecting groups prior to acquisition of photophysical data.

Figure Legends

Figure 1. Structures of the dipeptidomimetic analogues synthesized (**1** – **11**), and of FRET acceptor L-acridon-2-ylalanine (Acd).

Figure 2. Autoradiogram of a 15% SDS-polyacrylamide gel depicting the translation of modified GFPs from GFP mRNA, containing a UAG codon in position 66, in the presence of dipeptidomimetic (**1a**-**11a**)-$tRNA_{CUA}$ and an S-30 system prepared from ribosomal clone 010328R4 (lanes 3-13). Lanes 1 and 2 demonstrate the synthesis of full length GFP from the same mRNA in the presence of tyrosyl-$tRNA_{CUA}$ and non-acylated $tRNA_{CUA}$, respectively. Phosphorimager analysis was performed using an Amersham Biosciences Storm 820 equipped with ImageQuant version 5.2 software from Molecular Dynamics.

Figure 3. Comparison of emission profile of oxazoles **1a**, **3a** and **4a** (A, B and C, respectively) and thiazole **8a** (D), esterified to $tRNA_{CUA}$ (orange traces) versus incorporation in position 66 of GFP (blue traces). The concentrations of the activated tRNA solutions were adjusted to be roughly 3-4 fold greater than those of the proteins, to afford emission spectra of comparable intensity.

Figure 4. Fluorescence emission spectra of free oxazole **1a** (green trace); oxazole **1a** present in position 66 of GFP (blue trace) and oxazole **1a** esterified to $tRNA_{CUA}$ (orange trace) after excitation at 300 nm. All samples were present at 100 nM concentration in 25 mM Tris-HCl, pH 7.4, containing 0.25 M NaCl.

Figure 5. Fluorescence emission spectra of Boc-protected oxazole derivatives **63** (blue trace) and **12** (red trace). Both samples were present at 1.0 μM concentration in 25 mM Tris-HCl, pH 7.4, containing 0.5 M NaCl.

Figure 6. (A) Förster resonance energy transfer (FRET) between oxazole **1a** at position 66 of GFP and Acd at position 39 of the same protein. The sample was excited at 296 nm, affording a FRET signal at ~450 nm (blue trace). A control sample having **1a** at position 66, but no acceptor, exhibited no FRET when irradiated at 300 nm (Figure 4). Irradiation of the same sample at the excitation wavelength of Acd (370 nm) produced fluorescence emission centered at ~450 nm (orange trace). The sample was present at ~20 nM concentration in 25 mM Tris-HCl, pH 7.4, containing 0.25 M NaCl. (B) Model based on the X-ray crystal structure of green fluorescent protein (PDB 1GFL), showing the placement of oxazole **1a** in lieu of Tyr66, and Acd in place of Tyr39.

Figure 1

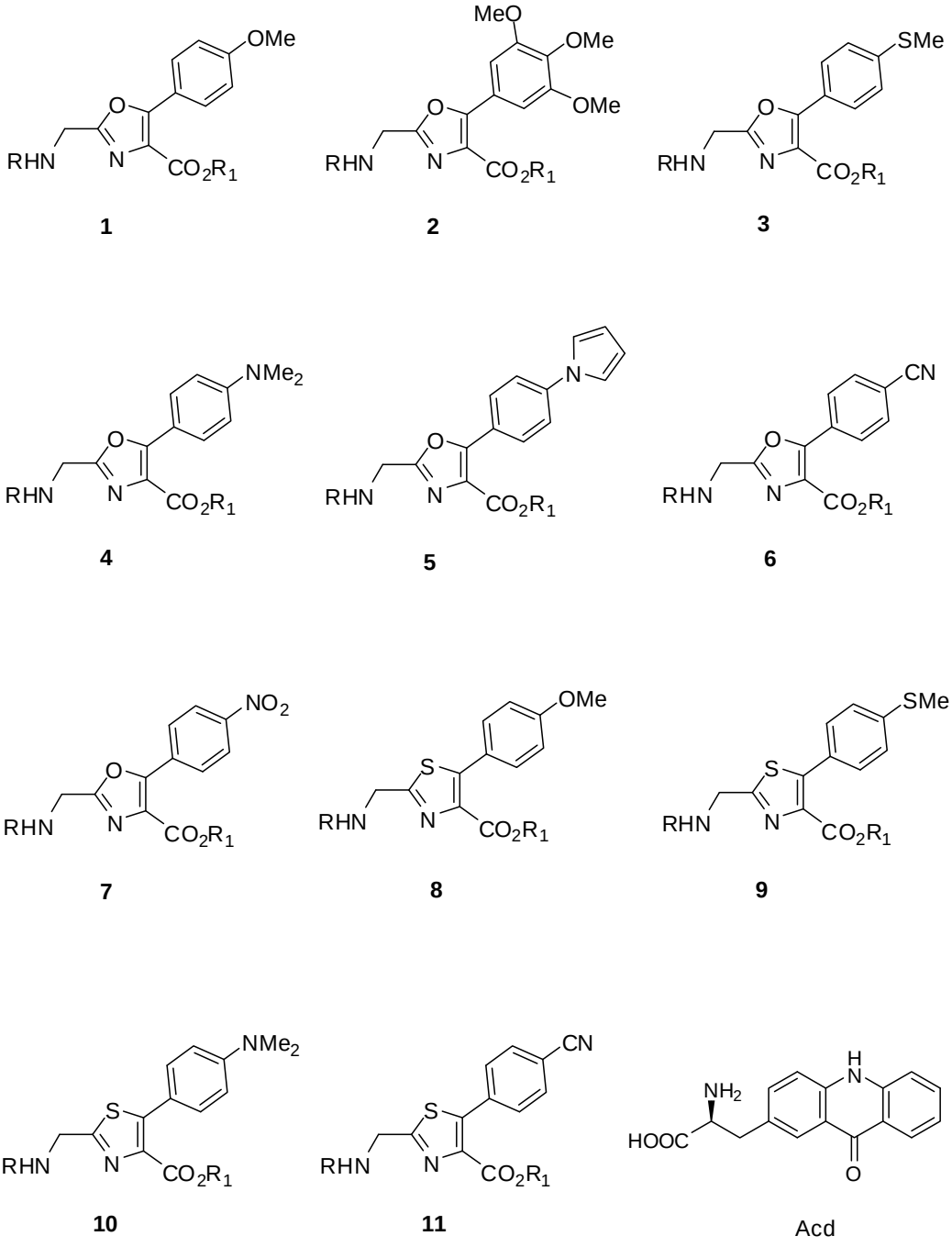

a R, R_1 = H

b R = 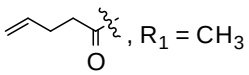 , R_1 = CH_3

Figure 2

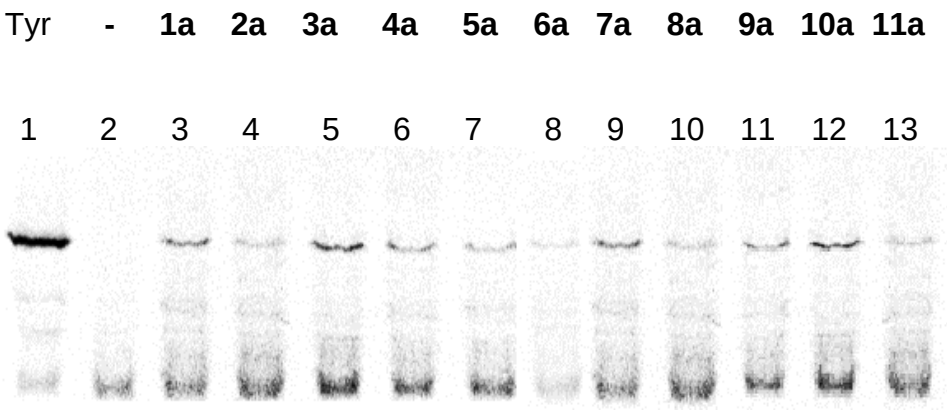

Figure 3

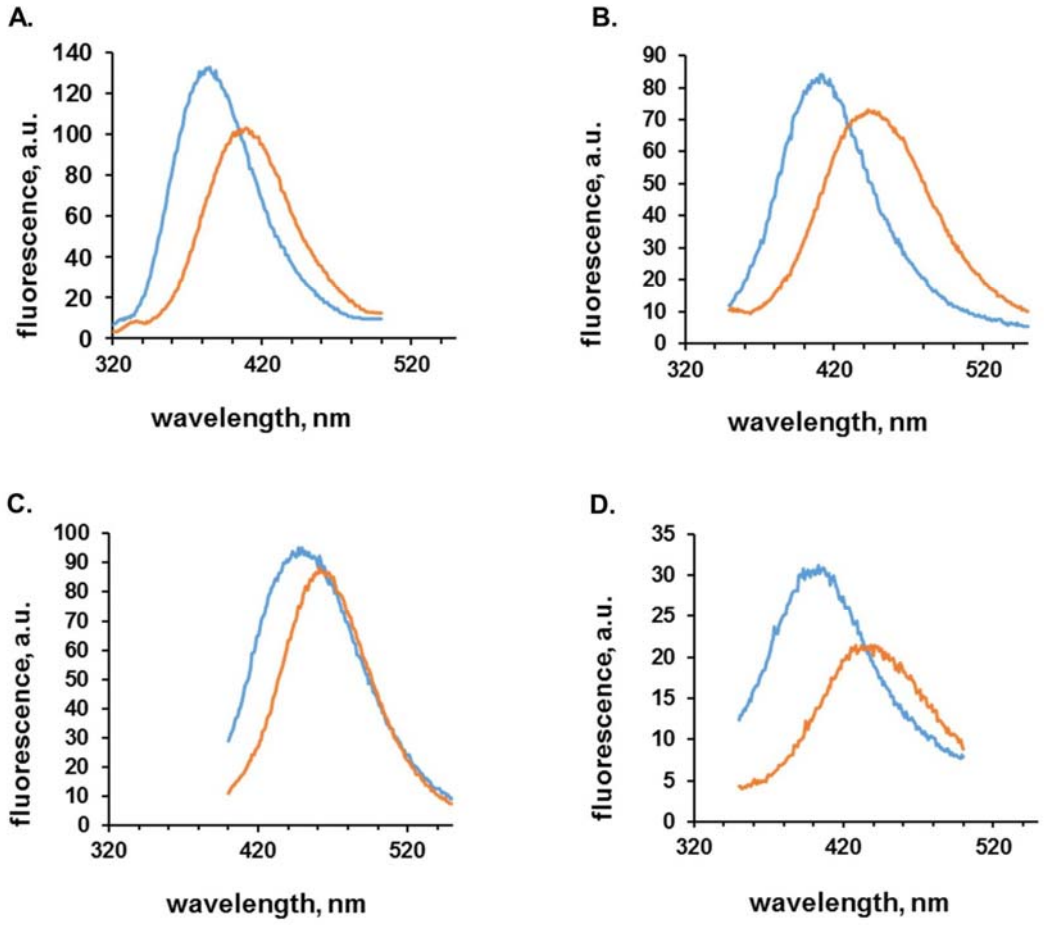
A.
fluorescence, a.u.
wavelength, nm
B.
fluorescence, a.u.
wavelength, nm
C.
fluorescence, a.u.
wavelength, nm
D.
fluorescence, a.u.
wavelength, nm

Figure 4

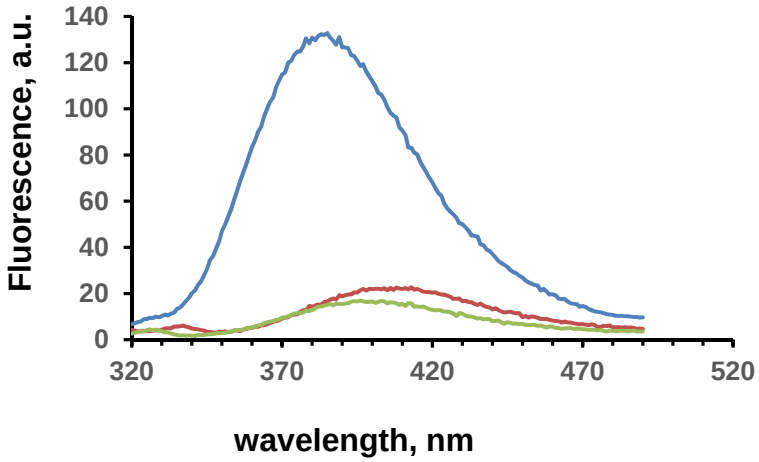
Fluorescence, a.u.
140
120
100
80
60
40
20
0
320
370
420
470
520
wavelength, nm

Figure 5

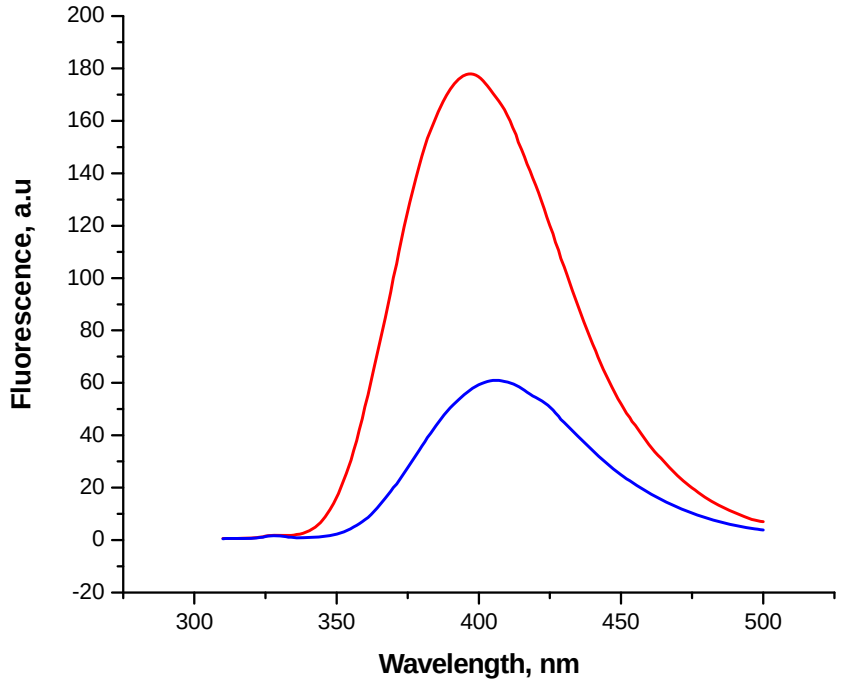
Fluorescence, a.u
200
180
160
140
120
100
80
60
40
20
0
-20
300
350
400
450
500
Wavelength, nm

Figure 6

A

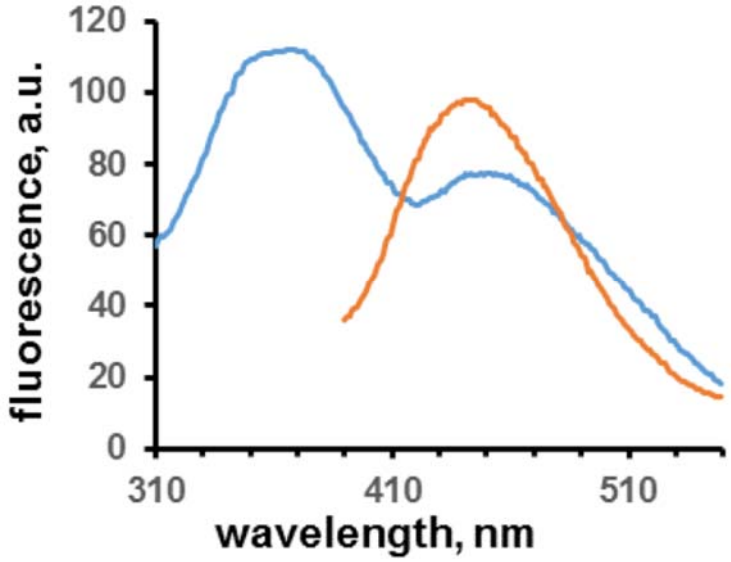
120
100
80
60
40
20
0
fluorescence, a.u.
310
410
510
wavelength, nm

B

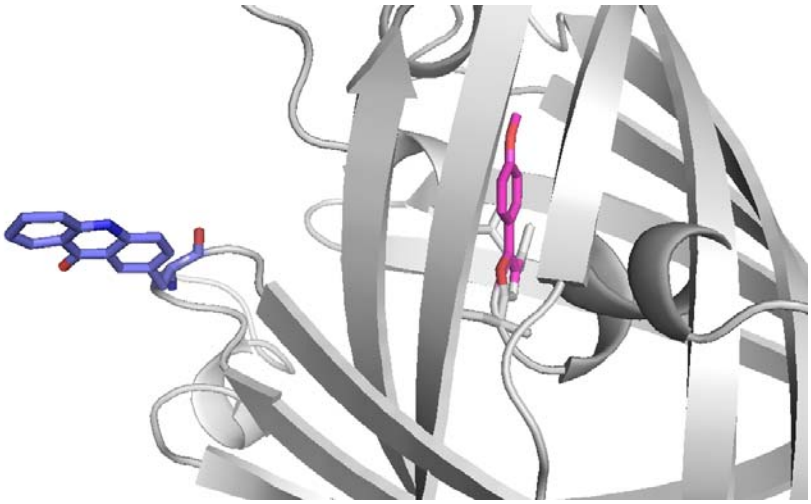

Scheme 1. Synthetic Route Employed for the Preparation of the pdCpA Derivative of Dipeptidomimetic Analogue 5a and its Attachment to a Suppressor $tRNA_{CUA}$

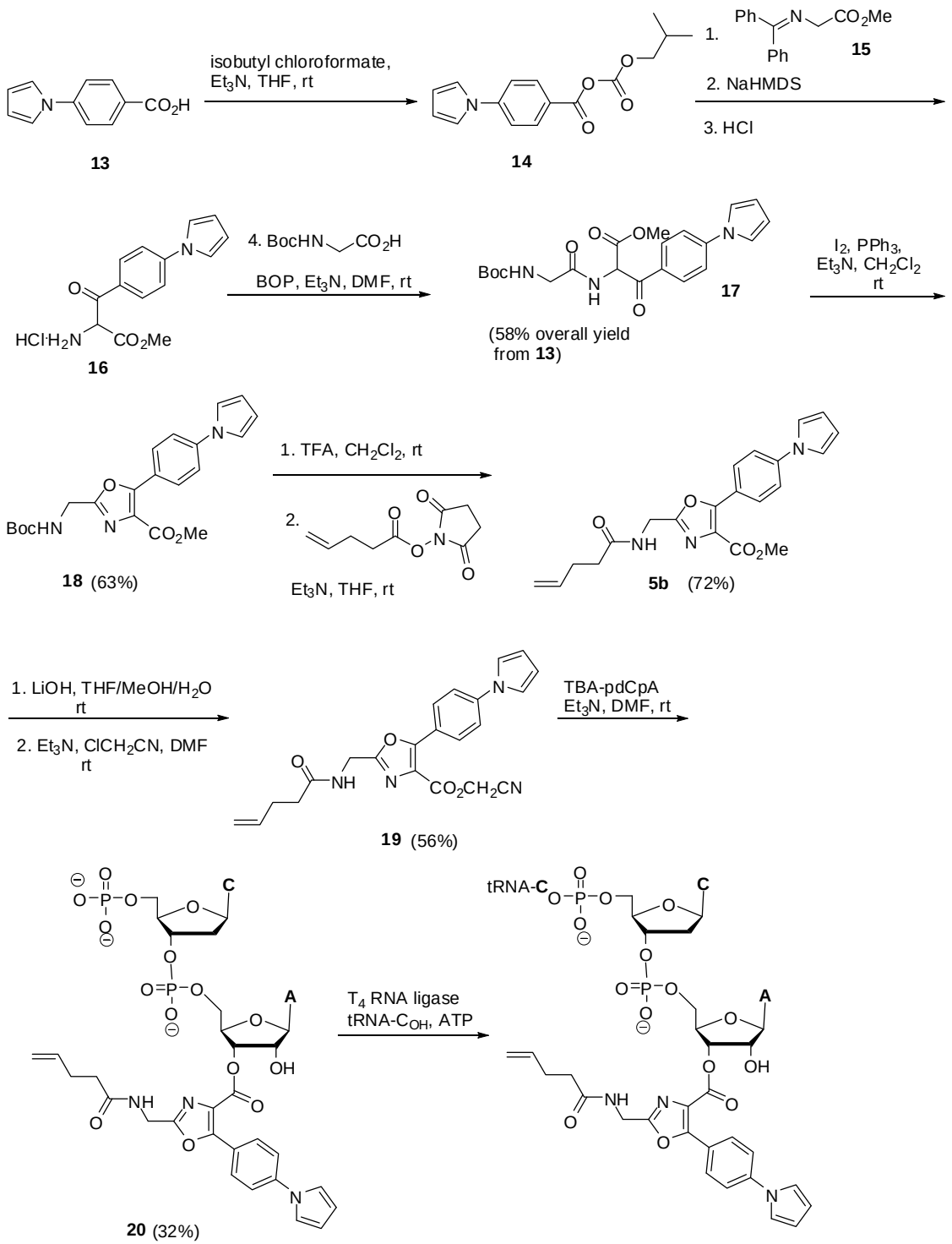

Scheme 2. Synthetic Route Employed for the Preparation of the *N*-Boc Methyl Ester Derivative of Fluorescent Peptide 12

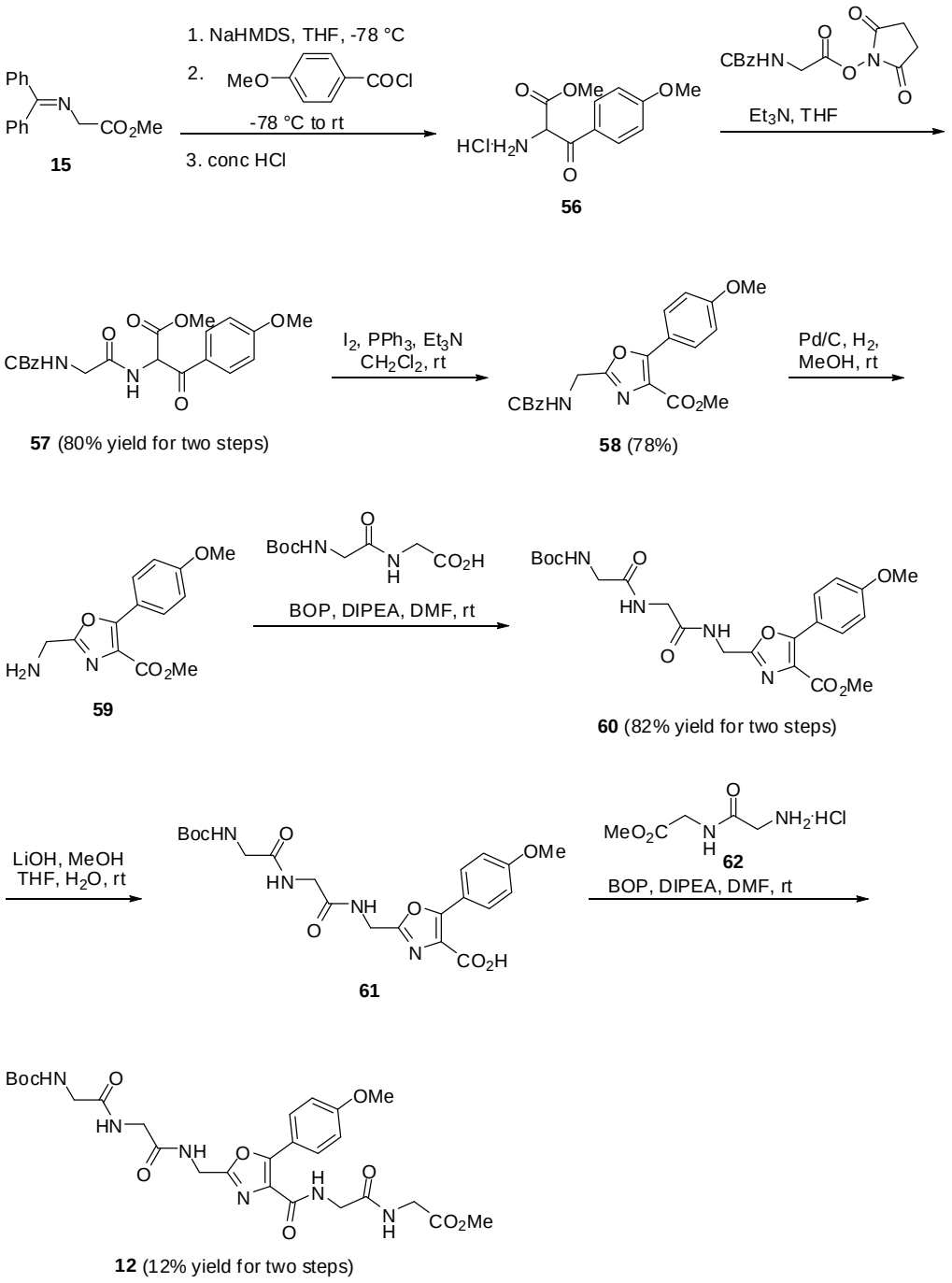

ToC Graphic

For Table of Contents Use only